

Comparative study of n-MgZnO/p-Si ultraviolet-B photodetector performance with different device structures

Y. N. Hou, Z. X. Mei,^{a)} H. L. Liang, D. Q. Ye, S. Liang, C. Z. Gu, and X. L. Du^{a)}

Beijing National Laboratory for Condensed Matter Physics, Institute of Physics, Chinese Academy of Sciences, Beijing 100190, China

(Received 5 May 2011; accepted 25 May 2011; published online 27 June 2011)

A comparative study of n-MgZnO/p-Si UV-B photodetector performance was carried out with different device structures. The experimental results demonstrate superior photoresponse characteristics of the p-n heterojunction detector against the Schottky type metal-semiconductor-metal counterpart, including a sharper cutoff wavelength at 300 nm, a larger peak photoresponsivity of 1 A/W, and a faster response speed. The role of built-in field and low interface scattering in p-n heterojunction is explored, and the energy band diagram of n-MgZnO/p-Si is employed to interpret the efficient suppression of visible light photoresponse from Si substrate, revealing the applicability of this heterostructure in fabrication of deep ultraviolet detectors. © 2011 American Institute of Physics. [doi:10.1063/1.3600789]

ZnO and related materials have been received more and more attention in recent decades due to their well-known versatile functionality in device applications.^{1–6} Mg_xZn_{1-x}O alloys with tunable band gaps are especially promising active components in ultraviolet (UV) light emitters,⁷ UV detectors,^{6,8} and other UV-range heterostructure devices.⁹ Among these applications, UV detection has a significantly huge market both in civil and military areas, such as missile plume early warning and flame/engine control.^{10,11} Considering its low growth temperature feature (<450 °C), MgZnO UV detector will become more competitive and practical when integrated with the well-developed Si microelectronic technologies, which suggests the urgent need for design of MgZnO UV detectors on Si substrates.

By far, most MgZnO UV detectors ever reported were fabricated in Schottky or photoconductive type device structures on sapphire substrates^{8,11–14} and only a few on silicon substrates.^{15–17} The shortest cutoff wavelength of MgZnO/Si photodetectors is around 300 nm with a not-steep photoresponse curve.¹⁷ A big challenge of high-quality epitaxial MgZnO film growth on Si greatly hampered the progress on this research field. In this case, it is not likely to carry out a systematic study of the optoelectronic properties of the detectors, not to mention the influence of device structures on detector performance, which is very important for understanding of the device physics.

We have developed a unique technique to engineer the interface of wurtzite MgZnO (0001)/Si (111) by radio-frequency plasma assisted molecular beam epitaxy (rf-MBE), where the deposition of a thin Be layer followed by oxidation was adopted to efficiently prevent the formation of amorphous SiO₂ layer and serve as a good template for epitaxial growth of MgZnO with high Mg content.¹⁸ The epitaxial relationship was determined as [0001]_{MgZnO}//[0001]_{BeO}//[111]_{Si} and [11-20]_{MgZnO}//[11-20]_{BeO}//[11-2]_{Si}. More growth details can be found elsewhere.¹⁸ In this letter, the n-MgZnO (0001)/p-Si (111) heterostructure was applied to fabricate

solar UV-B ($\lambda < 320$ nm) detectors with two different device structures, i.e., a vertical p-n heterojunction diode (labeled as device A) and a planar metal-semiconductor-metal (MSM) Schottky diode (labeled as device B). A comparative study of the optoelectronic properties for the two types of devices was then carried out, via the current-voltage (*I-V*), spectra response, and transient response measurements. Based on the experimental results, an energy band diagram of n-MgZnO/p-Si heterojunction was proposed to interpret the efficient suppression of visible light photoresponse from Si substrate in device A.

The single crystalline wurtzite MgZnO (0001) film was synthesized on a p-type Si (111) substrate by rf-MBE which was equipped with high purity elemental sources. To avoid Si surface oxidation, a Be layer with a thickness around 3 nm was firstly deposited, followed by an oxidation process. Growth of a quasi-homo MgZnO buffer layer (~20 nm) and a high Mg content MgZnO epilayer (350 nm) was subsequently carried out on the formed BeO layer.¹⁹ The optical bandgap and Mg content of the epilayer is 4.13 eV and 40%, respectively. The solar UV-B detectors were then fabricated by standard optical photolithography and lift-off technique. Ti (10 nm)/Au (50 nm) was deposited to form metal contact to n-MgZnO by thermal evaporation and indium as the back contact to p-Si. To increase the heterojunction detector's optical active area and promote the carriers collection efficiency, comb electrodes were used with 300 μm length, 5 μm width, and 15 μm gap [see the photograph in Fig. 1(a)]. The finger electrodes of MSM detectors were defined as 300 μm long and 5 μm wide with 5 μm gap [Fig. 1(b)]. Semiconductor parameter analyzer (Keithley 6487 picoammeter) was employed for *I-V* characterization. The spectra response was performed using the SpectraPro-500i (Acton Research Corporation) optical system with a 75 W Xe-arc lamp combined with a 0.5 m monochromator as the light source.

I-V curves of the two devices are shown in Fig. 1(c) with dot and triangle symbols, respectively. For device A, the rectification ratio is 147 under ± 3 V, indicating a good quality of the heterojunction. The ideality factor is calculated as 7.9 by fitting the curve with Sah-Noyce-Shockley model.

^{a)}Authors to whom correspondence should be addressed. Electronic addresses: zxmei@aphy.iphy.ac.cn and xldu@aphy.iphy.ac.cn.

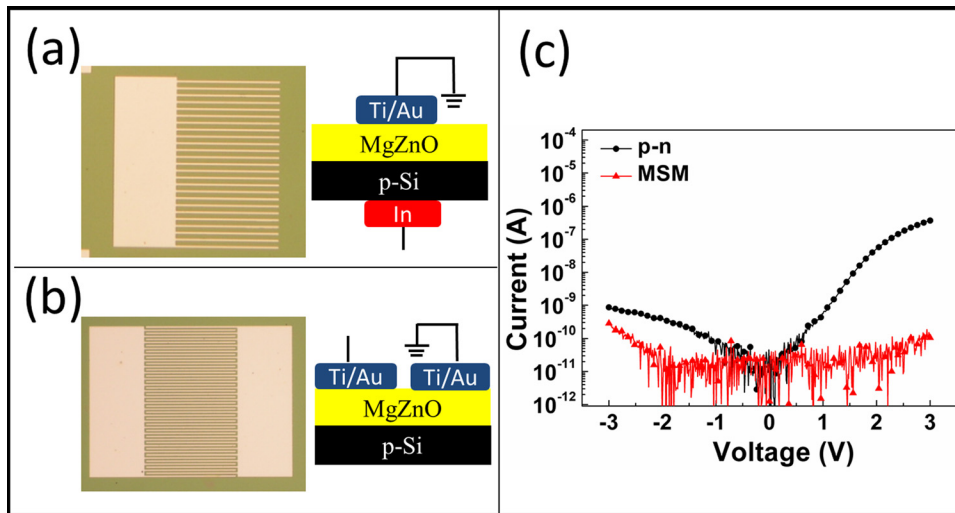


FIG. 1. (Color online) (a) Optical photograph and structure diagram of n-MgZnO/p-Si heterojunction UV-B detectors, (b) optical photograph and structure diagram of MSM MgZnO UV-B detectors on Si substrate, and (c) I - V characteristics of the two types of detectors.

Such a large ideal factor results from the series Schottky barrier formed by Ti/Au-MgZnO contact since the In-Si contact is confirmed Ohmic (not shown here). In contrast, the I - V curve of device B obviously shows a typical MSM type, and the dark current at reverse bias is much lower than device A. This difference comes from the different extent of electron scattering by thread dislocations, charged defects, and crystal lattice, since electrons need to transport a $5 \mu\text{m}$ transverse distance in device B while only a $0.3 \mu\text{m}$ longitudinal distance in device A.

Figure 2 shows the photoresponse performance of devices A and B at reverse 3 V bias. A sharp cutoff wavelength at 300 nm can be clearly recognized for both the devices, which agrees well with the optical bandgap of MgZnO epilayer. A shoulder response at 353 nm in device B originates from quasi-homo MgZnO buffer layer, which has a same level with the dark response and cannot be recognized in device A. Note that the peak photoresponsivity of device A (1 A/W) is one order of magnitude larger than that of device B (0.1 A/W), which indicates a lower extent of electron scattering and high efficiency in the separation of photo-generated carriers by the large longitudinal built-in electric field in device A. Note that the UV to visible light rejection ratio for device A can reach two orders of magnitude without the existence of insulator barrier between MgZnO and Si to suppress the visible response from Si substrate, which is much better than n-ZnO/p-Si heterostructure.²⁰ Our results suggest that the design of deep UV detectors may be simplified by using n-MgZnO/p-Si

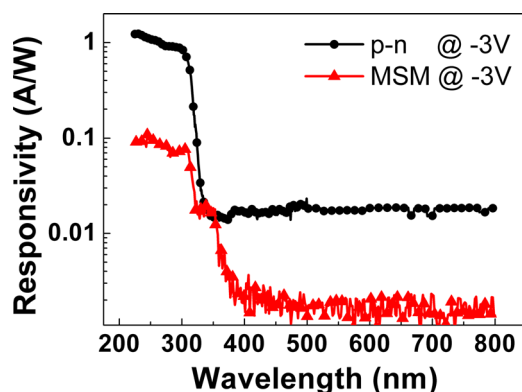


FIG. 2. (Color online) Spectra response of the two detectors.

heterojunctions, which are well suitable for solar UV-B monitoring and even working in quasi solar-blind UV region.^{21,22}

The time dependence of photocurrent properties were studied with the two device structures by using periodic 254 nm illumination from a UV lamp (Fig. 3). It can be seen that when the UV illumination is off, photocurrent of device A quickly returned to its initial value [Fig. 3(a)] while the value of device B can hardly reset due to the influence of persistent photocurrent (PPC) [Fig. 3(b)]. Since the two types of devices were fabricated with the same film sample, the PPC cannot be ascribed to the surface adsorption as previously reported on ZnO nanowires.²³⁻²⁵ In addition, the decay time of a similar MSM MgZnO detector on sapphire substrate we fabricated are about several hundreds of nanoseconds.⁸ Hence, the most possible reason for the PPC we observed is the MgZnO/Si interface states, which gradually release captured carriers and cause a PPC. Most of the photo-generated carriers are captured by the interface defects at UV-on stage since the carrier transportation in device B is in transverse direction. When device A is under UV illumination, however, the photo-generated carriers near the interface are separated

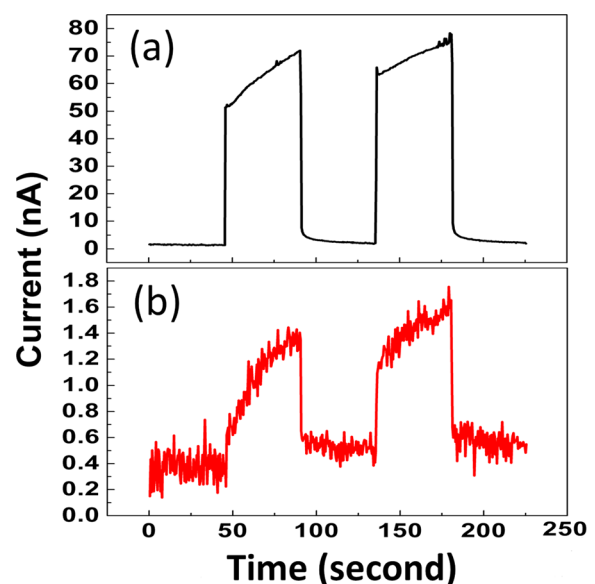


FIG. 3. (Color online) Time-dependent response of the photocurrent of device A (a) and device B (b) under periodic 254 nm illumination.

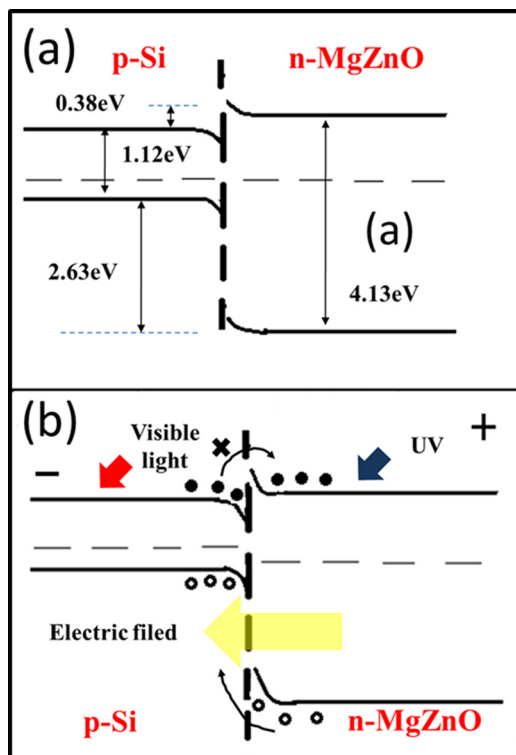


FIG. 4. (Color online) The energy-band diagram of n-MgZnO/p-Si heterojunction (a) under equilibrium condition and (b) under illumination at 3 V reverse bias.

immediately and drift to the electrodes under the force of the strong longitudinal electric field. The interface defects have little effect on the photo-generated carriers and the PPC can be therefore avoided.

The experimental results indicate a superior device performance of the p-n heterojunction detector compared with its MSM counterpart. To interpret the principle of the n-MgZnO/p-Si heterojunction detector, the energy band diagram was proposed according to Anderson-Shockley model as shown in Fig. 4. The electron affinity (χ) and band gap for Si and MgZnO are taken as 4.05 and 3.67 eV and 1.12 and 4.13 eV, respectively.⁷ The band offsets was hence determined as $\Delta E_C = \chi_{(\text{Si})} - \chi_{(\text{MgZnO})} = 0.38$ eV and $\Delta E_V = E_{g(\text{MgZnO})} - E_{g(\text{Si})} - \Delta E_C = 2.63$ eV. Under thermal equilibrium condition, the depletion region was formed both in Si and MgZnO sides due to the carrier diffusion [Fig. 4(a)]. The band bending at a reverse electric field is shown in Fig. 4(b). Considering the very small thickness of BeO interfacial layer (~ 3 nm), this layer cannot serve as an efficient barrier to block the photo-generated carriers like the case of MgO and SiO₂, which have larger dielectric coefficients than BeO.^{20,26}

When the device is under UV illumination, photo-generated holes in MgZnO layer will easily drift to the valence band of Si, generating a UV photocurrent. However, the photo-generated electrons in Si substrate by visible light were efficiently blocked by the conduction band offset ΔE_C of 0.38 eV, which recombine with holes without drifting into MgZnO side. In this case, the visible light response from Si substrate is efficiently suppressed by the natural band offset in the heterostructure. From this point of view, it is promising to fabricate n-MgZnO/p-Si heterojunction deep UV detectors with high performance.

In summary, a comparative study of p-n heterojunction and MSM UV-B detectors based on n-MgZnO film grown on p-Si (111) substrate has been carried out. The heterojunction detector performed much better than the MSM counterpart both in photoresponsivity and response speed, which benefits from the strong built-in electrical field and less influence of interface defects. The energy band diagram was adopted to illuminate the principle of the detectors, suggesting the n-MgZnO/p-Si heterojunction UV-B detector can work without the insertion of insulator barrier to suppress the visible response from the substrate. Based on these results, we predicted it is applicable to fabricate deep UV detectors with high Mg component MgZnO epitaxial films on Si substrate.

This work was supported by the National Science Foundation (Grant Nos. 61076007, 50532090, 60606023, 50825206), the Ministry of Science and Technology (Grant Nos. 2007CB936203, 2009CB929400, 2009AA033101, 2011CB302002) of China, and Chinese Academy of Sciences.

¹F. Tuomisto, V. Ranki, K. Saarinen, and D. C. Look, *Phys. Rev. Lett.* **91**, 205502 (2003).

²C. Coskun, D. C. Look, G. C. Farlow, and J. R. Sizelove, *Semicond. Sci. Technol.* **19**, 752 (2004).

³J. J. Wu and S. C. Liu, *Adv. Mater.* **14**, 215 (2002).

⁴L. E. Greene, M. Law, D. H. Tan, M. Montano, J. Goldberger, G. Somorjai, and P. D. Yang, *Nano Lett.* **5**, 1231 (2005).

⁵A. Tsukazaki, A. Ohtomo, T. Onuma, M. Ohtani, T. Makino, M. Sumiya, K. Ohtani, S. F. Chichibu, S. Fuke, Y. Segawa, H. Ohno, H. Koinuma, and M. Kawasaki, *Nature Mater.* **4**, 42 (2005).

⁶X. L. Du, Z. X. Mei, Z. L. Liu, Y. Guo, T. C. Zhang, Y. N. Hou, Z. Zhang, Q. K. Xue, and A. Y. Kuznetsov, *Adv. Mater.* **21**, 4625 (2009).

⁷A. Ohtomo, M. Kawasaki, I. Ohkubo, H. Koinuma, T. Yasuda, and Y. Segawa, *Appl. Phys. Lett.* **75**, 980 (1999).

⁸Y. N. Hou, Z. X. Mei, Z. L. Liu, T. C. Zhang, and X. L. Du, *Appl. Phys. Lett.* **98**, 103506 (2011).

⁹A. Tsukazaki, A. Ohtomo, T. Kita, Y. Ohno, H. Ohno, and M. Kawasaki, *Science* **315**, 1388 (2007).

¹⁰I. Takeuchi, W. Yang, K. S. Chang, M. A. Aronva, T. Venkatesan, R. D. Vispute, and L. A. Bendersky, *J. Appl. Phys.* **94**, 7336 (2003).

¹¹R. Ghosh and D. Basak, *J. Appl. Phys.* **101**, 113111 (2007).

¹²S. S. Hullavarad, S. Dhar, B. Varughese, I. Takeuchi, T. Venkatesan, and R. D. Vispute, *J. Vac. Sci. Technol. A* **23**, 982 (2005).

¹³W. Yang, R. D. Vispute, S. Choopun, R. P. Sharma, T. Venkatesan, and H. Shen, *Appl. Phys. Lett.* **78**, 2787 (2001).

¹⁴S. P. Chang, S. J. Chang, Y. Z. Chiou, C. Y. Lu, T. K. Lin, Y. C. Lin, C. F. Kuo, and H. M. Chang, *Sens. Actuators A* **140**, 60 (2007).

¹⁵M. Fujita, M. Sasajima, Y. Deesirapipat, and Y. Horikoshi, *J. Cryst. Growth* **278**, 293 (2005).

¹⁶W. Yang, S. S. Hullavarad, B. Nagaraj, I. Takeuchi, R. P. Sharama, T. Venkatesan, R. D. Vispute, and H. Shen, *Appl. Phys. Lett.* **82**, 3424 (2003).

¹⁷K. Koike, K. Hama, I. Nakashima, G. Y. Takada, K. I. Ogata, S. Sasa, M. Inoue, and M. Yano, *J. Cryst. Growth* **278**, 288 (2005).

¹⁸H. L. Liang, Z. X. Mei, Q. H. Zhang, L. Gu, S. Liang, Y. N. Hou, D. Q. Ye, C. Z. Gu, and X. L. Du, *Appl. Phys. Lett.* **98**, 221902 (2011).

¹⁹Z. L. Liu, Z. X. Mei, T. C. Zhang, Y. P. Liu, Y. Guo, X. L. Du, A. Hallen, J. J. Zhu, and A. Yu. Kuznetsov, *J. Cryst. Growth* **311**, 4356 (2009).

²⁰T. C. Zhang, Y. Guo, Z. X. Mei, C. Z. Gu, and X. L. Du, *Appl. Phys. Lett.* **94**, 113508 (2009).

²¹W. B. Grant, E. V. Browell, N. S. Higdon, and S. Ismail, *Appl. Opt.* **30**, 2628 (1990).

²²H. G. Li, G. Wu, H. Z. Chen, and M. Wang, *Org. Electron.* **12**, 70 (2010).

²³J. B. K. Law and T. L. Thong, *Appl. Phys. Lett.* **88**, 133114 (2006).

²⁴Y. Z. Jin, J. P. Wang, B. Q. Sun, J. C. Blakesley, and N. C. Greenham, *Nano Lett.* **8**, 1649 (2008).

²⁵J. Zhou, Y. D. Gu, Y. F. Hu, W. J. Mai, P. H. Yeh, G. Bao, A. K. Sood, D. L. Polla, and Z. L. Wang, *Appl. Phys. Lett.* **94**, 191103 (2009).

²⁶H. D. Um, S. A. Moiz, K. T. Park, J. Y. Jung, S. W. Jee, C. H. Ahn, D. C. Kim, H. K. Cho, D. W. Kim, and J. H. Li, *Appl. Phys. Lett.* **98**, 033102 (2011).